Next-generation sequencing studies guide the design of pyrrole-imidazole polyamides with improved binding specificity by the addition of β-alanine.

AUTHOR(S):

Anandhakumar, Chandran; Li, Yue; Kizaki, Seiichiro; Pandian, Ganesh N; Hashiya, Kaori; Bando, Toshikazu; Sugiyama, Hiroshi

CITATION:

Anandhakumar, Chandran ...[et al]. Next-generation sequencing studies guide the design of pyrrole-imidazole polyamides with improved binding specificity by the addition of β-alanine.. ChemBioChem 2014, 15(18): 2647-2651

ISSUE DATE:

2014-11-04

URL:

http://hdl.handle.net/2433/200257

DOI: ((will be filled in by the editorial staff))

Next-Generation Sequencing Studies Guide the Design of Pyrrole-Imidazole Polyamides with Improved Binding Specificity by the Addition of β-alanine

*Chandran Anandhakumar, Yue Li, Seiichiro Kizaki, Ganesh N. Pandian, Kaori Hashiya, Toshikazu Bando, and Hiroshi Sugiyama**

Abstract: *The identification of binding sites for small molecules in the genome space is important for various applications. Previously, we demonstrated rapid transcriptional activation by our small molecule SAHA-PIPs. However, it was not clear whether the strong biological effects exerted by SAHA-PIP were due to its binding specificity. Here, we used high-throughput sequencing (Bind-n-seq) to identify the binding specificity of SAHA-PIPs. Firstly sequence specificity bias was determined with SAHA-PIPs (**3** and **4**), which showed enhanced 6-bp sequence-specific binding compared with hairpin PIPs (**1** and **2**). This finding allowed us to investigate the role of β-alanine that links SAHA with PIP, which led to the design of ββ-PIPs (**5** and **6**). ββ-PIPs showed enhanced binding specificity. Overall, we demonstrated the importance of β-moieties for the binding specificity of PIPs, and the utilization of cost-effective high-throughput screening of these small molecules to the minor groove*

Dysregulation of gene expression is a major cause of many diseases. Global gene expression is governed by transcriptional regulation, and genetic and epigenetic machinery plays major roles in this. Alteration of the epigenetic mechanism can provide targeted gene regulation and cellular reprogramming, and could enable the development of artificial genetic switches, governed by DNA-binding small molecules, which could bring back otherwise irredeemable dysfunctions connected with defective transcriptional/epigenetic machinery.[1] Hairpin *N*-methylpyrrole (P)–*N*-methylimidazole (I) polyamides (PIPs) are a class of small molecule that can bind in the minor groove of DNA[2] and can recognize each of the four Watson–Crick base pairs.[3] When arranged side-by-side, I and P discriminate C·G from G·C base pairing,[2] whereas the P and P pair can recognize both A·T and T·A.[4]

Chromatin-modifying enzymes can alter transcriptional regulation randomly by epigenome modification.[5] Previously, we linked PIP to an epigenetically active histone deacetylase (HDAC) inhibitor (SAHA) to generate SAHA-PIP[6, 7] and demonstrated the effect of SAHA-PIPs in mouse fibroblasts to induce differential activation of pluripotent stem cell-associated genes.[7] This study demonstrated the efficiency of SAHA-PIP in intervening in transcriptional activation and showed that the compound may activate the silent gene system in somatic cells. Our recent report on the microarray analysis of a SAHA-PIP library revealed that such compounds can trigger a unique set of gene clusters in human dermal fibroblast (HDF) cells.[8] However, whether the strong biological effects exhibited by SAHA-PIP were due to its binding specificity in a broad context was unclear.

Recently, the binding sites of hairpin PIPs in DNA at the genome level were reported.[9] In this approach, termed Bind-n-seq, PIPs were tagged with biotin and the bound DNA was analyzed by high-throughput sequencing methods.[9] Although the PIPs bound to the DNA with canonical pairing rules as predicted, some PIPs were identified with the reverse binding orientation.[9]

In this study, we identify the high-affinity binding sites of the previously reported germ cell gene activating SAHA-PIP K[10] and its structurally similiar counterpart SAHA-PIP I[8] that activate an entirely different set of developmental genes (Figure 1). By using the Bind-n-seq approach, we could identify the binding specificity of SAHA-PIP I (**3**) and SAHA-PIP K (**4**) in a broad context of oligo libraries. Both compounds showed high-affinity binding compared with PIP I (**1**) and PIP K (**2**) (PI polyamide without SAHA). This prompted us to redesign SAHA-PIP and replace the SAHA moiety with β-alanine (the β-moiety) in the non-core binding region of the 10-ring hairpin polyamide. The results showed that the β-moiety enforces binding of PIP in the closed form.

[*] C. Anandhkumar, Y. Li, S. Kizaki, K. Hashiya, T. Bando, Prof. H. Sugiyama
Department of Chemistry, Graduate School of Science Kyoto University, Kitashirakawa-oiwakecho, Sakyo-ku, Kyoto 606-8502
E-mail: hs@kuchem.kyoto-u.ac.jp
G. N. Pandian, Prof. H. Sugiyama
Institute for Integrated Cell-Material Sciences (WPI-iCeMS) Kyoto University, Yoshida-ushinomiyacho, Sakyo-ku, Kyoto 606-8501 (Japan).

[**] This research was supported by the Ministry of Education, Culture, Sports, Science and Technology (MEXT) of Japan, administrated by the Japan Society for the Promotion of Science (JSPS).
We thank JEES Mitsubishi Corporation Scholarship for supporting C. Anandhakumar.

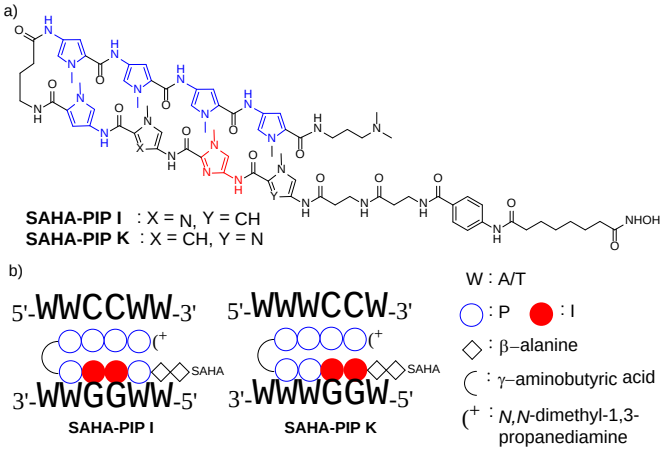

Figure 1. a) Chemical structures, and b) DNA sequence-specific binding models of SAHA-PIP I and K.

Application of the epigenetically active and DNA-binding SAHA-PIPs I and K relies largely on high-affinity sites. SAHA-PIPs are expected to bind in the minor groove of DNA according to well-defined pairing rules (N-terminal to C-terminal:5′-3′).[6] Meier et al. studied the sequence selectivity and canonical pairing rules of PIP-DNA binding in a broad sequence context using affinity purification coupled with massively parallel sequencing in an Illumina sequencer.[9] To characterize the binding specificity of the PIP derivatives, we carried out high-throughput sequencing (Bind-n-seq) studies in a randomized DNA sequence space to define the recognition motifs of PIPs and SAHA-PIPs (Figure 2).

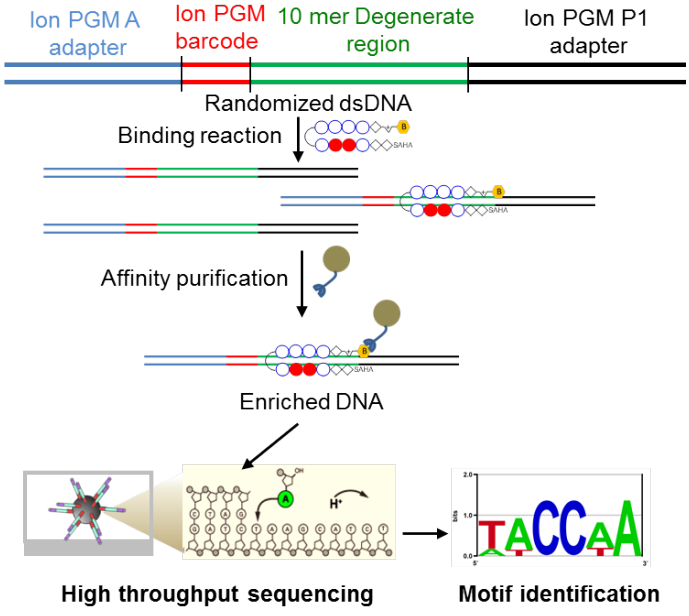

Figure 2. High-throughput sequencing based Bind-n-seq experimental design and binding motif discovery.

A small library of biotin-conjugated PIPs and SAHA-PIPs (**1**–**4**) (Scheme 1, **1**-**4**)was first synthesized (in the SAHA moiety of biotin-conjugated SAHA-PIPs (**3** and **4**), we used the methyl ester instead of hydroxamic acid for synthetic convenience. This change was not expected to affect the DNA-binding affinity of the SAHA-PIPs because SAHA does not bind DNA. Synthesis details are provided in the supporting information), and allowed to bind with 10-bp randomized DNA fragments equipped with an Ion PGM-compatible adapter sequence (for details of the design of the oligos and primer used to make duplex DNA, see the Supplementary Information). By using affinity purification, the enriched DNA sequences bound by the PIP derivatives were extracted and sequenced with an Ion PGM sequencer . After a quality check and adapter trimming of the sequenced reads, Bind-n-Seq analysis[11] revealed enrichment of "*k*-mer" (*k* = 6), and confirmed that the binding sites of **3** and **4** matched the canonical binding rule. Interestingly, **4** was found to bind in the forward orientation (N-terminal to C-terminal:5′-3′, Figure 3d), but it was difficult to determine the binding orientation of **3** (Figure 3c) because of its symmetrical binding site (5′-WWCCWW-3′ / 5′-WWGGWW-3′). The results obtained with **4** are significant because the PIPs have the ability to bind in both forward and reverse orientation and hence have a relatively large number of duplex DNA sites as potential targets. When the binding of **4** is principally in the forward orientation, then the number of potential target sites is reduced, which in turn suggests superior specificity over **2**. Motifs were identified by using the DREME[12a] and enoLOGOS[12b] algorithms, which are motif-binding programs developed to identify the short response elements typically bound by eukaryotic transcription

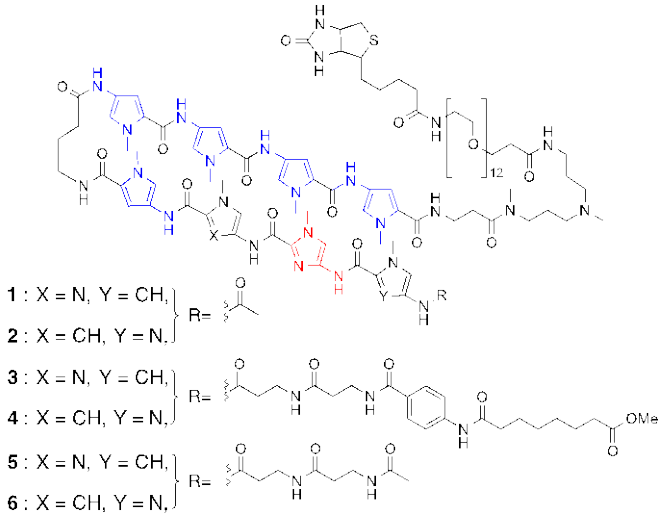

Scheme 1. a) Chemical structures **1**-**6**

factors. From the analysis described above, a graphical depiction of the strongest motif was generated for the highly enriched binding site of **1**–**4** (Figure 3a–3d); a table of enriched sequences is given in the Supplementary Information. Replicate quantification validated the high-affinity binding; for example, the enrichment of DNA sequences bound by **3** was highly reproducible (R^2 = 0.92 for two separate binding and enrichment experiments; Figure S1). The enriched sequence data and the similarity of enrichment between two different experiments are shown in the Supplementary Information.

The results of the massively parallel sequencing analysis Bind-n-seq showed that **3** and **4** (Figure 3c and 3d) had high-affinity binding toward the canonical binding sites. However, the results also showed that **1** and **2** bound with randomized DNA in an open conformation (Figure 3a and 3b). In addition to the SAHA moiety, **3** and **4** contain two β-alanine moieties (used to conjugate the SAHA with PIP) in the non-core binding machinery; compounds **1** and **2** lack these two β-moieties. The high-affinity binding of **3** and **4**

prompted us to investigate the role of the β-alanine moiety in the construction of hairpin PIP. To this end, we designed PIP derivatives **5** and **6** (corresponding to SAHA-PIPs without SAHA) (Scheme 1, **5**-**6**), having two β-alanine moieties in the non-core binding domain. Thus, ββ-PIP-biotin conjugates **5** and **6** were synthesized and subjected to binding reaction with randomized DNA with affinity purification followed by massively parallel sequencing.

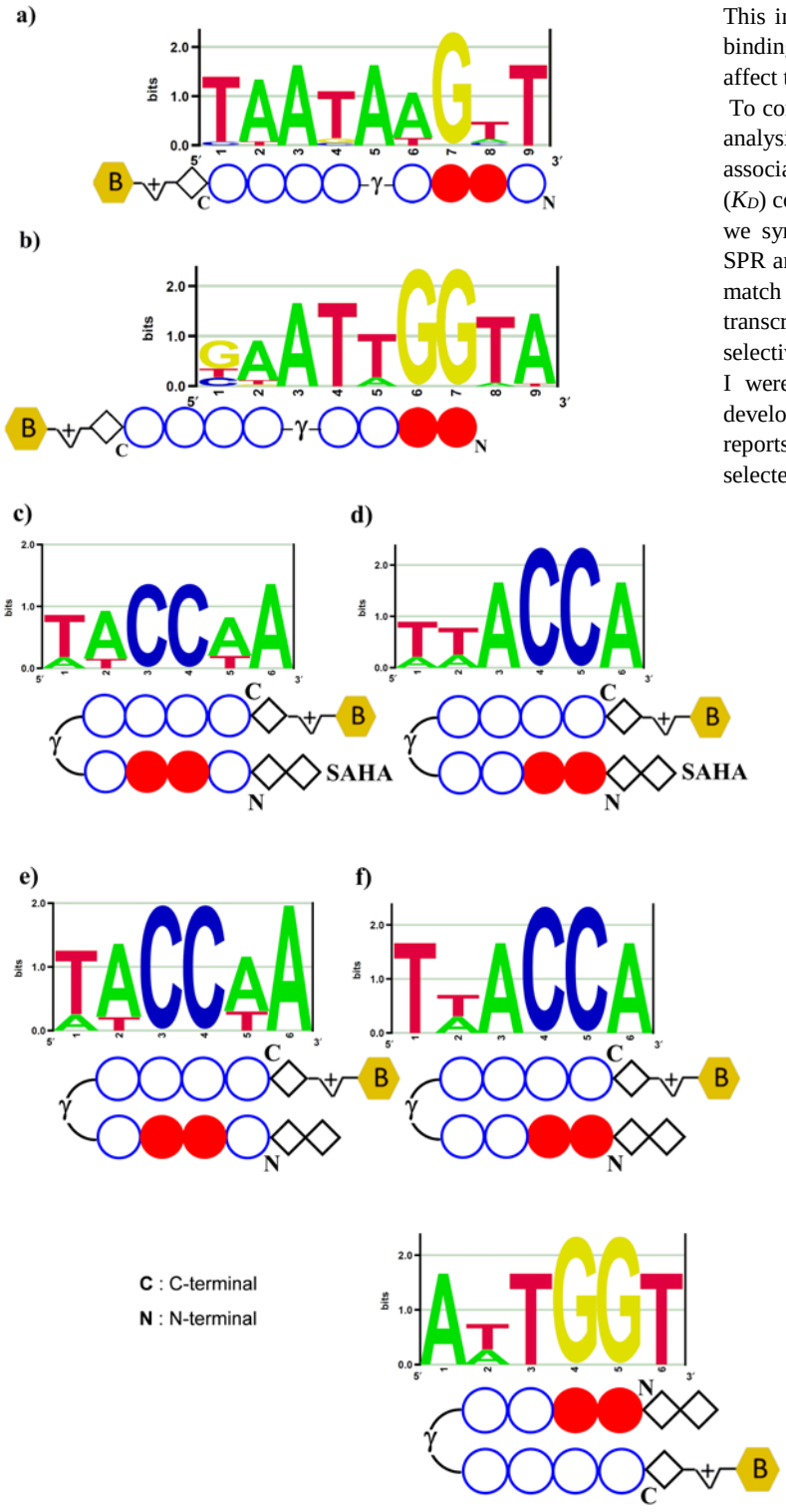

Figure 3. Structure of Polyamides binding region and its primary binding motifs identified using Bind-n-seq through next generation sequencing: (a) **1** (b) **2** (c) **3** (d) **4** (e) **5** (f) **6**.

Bind-n-seq data analyses were performed for sequence reads enriched by **5** and **6**. Assessment of the identified motifs (Figure 3e and 3f) revealed that the β-alanine moiety enforces high-affinity binding of the PIPs in the closed form. Compounds **5** and **6** bind with the WWCCWA and TWACCA/AWTGGT sites, respectively. Since we could not identify the binding orientation of **5**, we considered only the binding orientation of **6**. Interestingly, DNA motifs enriched after binding **6** revealed that this compound bound to the DNA with equal affinity of forward and reverse orientations. This investigation thus indicates that the β-alanine moiety induces binding of hairpin PIP in the closed form with DNA and does not affect the direction of binding.

To confirm the findings of Bind-n-seq analyses, we performed SPR analysis because previous reports have shown that the rates of association (k_a) and dissociation (k_d), and the dissociation constant (K_D) correlate well with the binding affinity.[13] For the SPR analysis, we synthesized PIPs **7**–**10** without biotin conjugates (Scheme 2). SPR analyses were performed with a Biacore X instrument with the match and mismatch DNA oligonucleotides from the human transcription factor sequences to identify whether PIP binding can selectively trigger human transcription factors[13]. SAHA-PIP K and I were shown to distinctively regulate the expression of silent developmental genes in human fibroblasts. Based on our previous reports, for **7** and **9** (similar binding sequence as SAHA-PIP I), we selected the match sequences in the promoter region of the gene encoding the developmental associated POU homeodomain [8] and for **8** and **10** (similar binding sequence as SAHA-PIP K), we selected the match (**8** and **10**) sequences in the promoter region of the gene encoding the germ cell associated *PIWIL 2* [10]. For checking the relative binding affinity, the match sequences of SAHA-PIP I (**7** and **9**) and K (**8** and **10**) were interchanged and used as the mismatch sequences. We compared the binding ability and efficiency of compounds **9** and **10** with those of **7** and **8** in the corresponding match and mismatch binding of DNA. The PIP derivatives were passed through a 5′-biotinylated hairpin DNA immobilized sensor chip by using a biotin–avidin system. The binding affinities of the PIP derivatives were measured by analyzing the data produced from the SPR method. Detailed assessment of the SPR dissociation constant (K_D) values showed that **9** and **10** had higher affinity toward the matching polyamide–DNA binding sites than **7** and **8**, with a K_D range of approximately 5–25-fold. These data correlate best with the binding sites identified by Bind-n-seq. The rates of association (k_a) and dissociation (k_d) and the dissociation constants (K_D) are shown in Table 1, and the sensorgrams are shown in the Supplementary Information (Figures S2 and S3). Although many methods are under development, the targeting of dsDNA in a genomic sequence perspective by using small synthetic molecules remains difficult. The structural composition of polyamides and DNA sequence-dependent structural variations may decrease the binding specificity of PIP derivatives to the desired specific DNA-binding sites. This study delivers a low-cost sequencing method for designing and screening of sequence-specific DNA-binding molecules with the standardized experimental conditions. We have shown that the addition of a SAHA moiety to the N-terminal of PIPs does not affect the canonical binding rule of polyamides in a wide sequence context. Thus, the HDAC inhibitor SAHA can be used in a sequence-specific manner with the assistance of polyamides as we reported earlier.[10]

Despite the finding that polyamides bind according to the canonical binding rule, we have identified that **1** and **2** (without SAHA) can also preferentially bind to DNA in an open conformation instead of in the hairpin form. This phenomenon was not observed for **3** and **4** (PIPs with SAHA), which prompted us to look in more detail at the features leading to polyamide binding in the closed form. Our investigation focused on the two N-terminal β-alanine moieties in

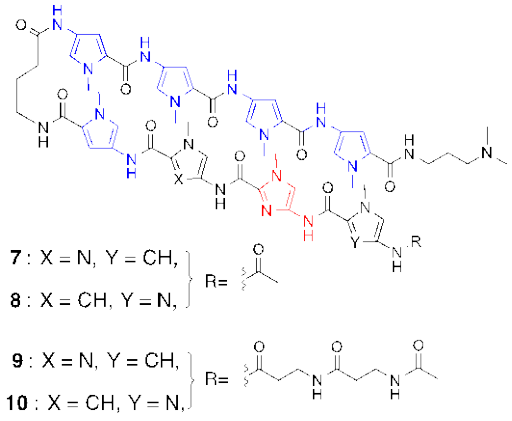

Scheme 2. Chemical structures **7-10**

the non-core binding machinery. Several biologically active polyamides with β-residues in the core binding sites have been reported, and the importance of β-residue placement in the core binding region of polyamides has been examined.[14] However, none of the studies investigated the effect of β-moieties in the N-terminal

Table 1. Binding affinities of polyamide **7-10**

polyamide	5'-Biotin labeled- GCGCCTTCCTTCCCCT$_T^T$ 3'- CGCGGAAGGAAGGGGT$_T^T$		5'-Biotin labeled- CGTCCTTTCCAGCAGT$_T^T$ 3'-GCAGGAAAGGTCGTC T$_T^T$		specificity
	K_D(M) match		K_D(M) 2-bp mismatch		
7 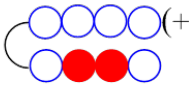	**1.2 x 10^{-7}**	$Ka(M^{-1}s^{-1})$ 1.4 x 10^5 $Kd(s^{-1})$ 1.6 x 10^{-2}	**1.8 x 10^{-7}**	$Ka(M^{-1}s^{-1})$ 1.0 x 10^5 $Kd(s^{-1})$ 1.8 x 10^{-2}	**1.5**
9 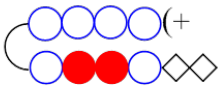	**2.8 x 10^{-8}**	$Ka(M^{-1}s^{-1})$ 1.2 x 10^6 $Kd(s^{-1})$ 3.3 x 10^{-2}	**1.4 x 10^{-7}**	$Ka(M^{-1}s^{-1})$ 1.6 x 10^5 $Kd(s^{-1})$ 2.1 x 10^{-2}	**5.0**
	K_D(M) 2-bp mismatch		K_D(M) match		
8 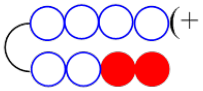	**1.1 x 10^{-7}**	$Ka(M^{-1}s^{-1})$ 1.4 x 10^5 $Kd(s^{-1})$ 1.6 x 10^{-2}	**1.5 x 10^{-8}**	$Ka(M^{-1}s^{-1})$ 2.5 x 10^5 $Kd(s^{-1})$ 3.7 x 10^{-3}	**7.7**
10 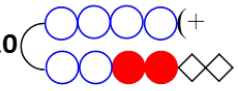	**6.5 x 10^{-8}**	$Ka(M^{-1}s^{-1})$ 2.6 x 10^5 $Kd(s^{-1})$ 1.7 x 10^{-2}	**2.5 x 10^{-9}**	$Ka(M^{-1}s^{-1})$ 1.3 x 10^6 $Kd(s^{-1})$ 3.1 x 10^{-3}	**26**

non-core binding machinery. We studied the Bind-n-seq offered high-affinity binding of polyamides with ββ-PIP derivatives **5** and **6** and established which sequences are enriched by ββ-PIPs with a high-throughput sequencing method. The identified motifs clearly indicate that the N-terminal β-residue can restore the forward polyamide-binding specificity. This conclusion was further supported by the results of SPR analysis. Although the ββ-PIP derivatives can restore the forward binding affinity, the motifs identified by **6** show both forward and reverse binding orientations, in which the core binding N-terminal of the polyamide is *N*-methylimidazole (I). This result suggests that the ββ-residues direct the polyamide to bind in the hairpin form. Previous studies have shown[9a] that the replacement of a β-amino–GABA linker with an α-amino–GABA linker can restore the forward binding of polyamides. Our results with **5** show that the N-terminal non-core β-residues can also restore the high forward binding affinity of polyamides, in which the core binding N-terminal of the polyamide is *N*-methylpyrrole (P). Further studies need to be carried out to confirm the exact number of β-residues required to restore the forward orientation of polyamide binding.

Experimental Section

Bind-n-seq

Previously reported Bind-n-Seq experiments[9] and subsequent analysis to evaluate small molecule binding affinity towards specific DNA sequences in a broad context sequence pool were customized with the modifications suitable for Ion torrent PGM sequencer. The scheme involves the following three major steps, 1) Synthesis of biotinylated PIPs**,** and randomized oligonucleotides with high-throughput sequencing platform specific adapters (Ion torrent PGM) (sequence details were given in supporting information). Adapter ligated oligonucleotides (3μM) were duplexed by primer extension with adapter specific primer 1 (9μM) in 25μL reaction contain 2x goTag PCR master mix with 2mM Mg^{2+}. Reactions were performed at 95°C (3 min), 60°C (2 min), 70°C (5 min) and then 4°C using Bio-Rad thermocycler. Biotin conjucated PIPs (100nM) were allowed to equilibrate with duplex random oligonucleotides for 14 hrs followed by Streptavidin M-280 Dynabeads (Beads were prepared based on the previous report[9]) separation of the bound and unbound sequences using affinity purification. 2) Polyamides-enrichment recovered DNA was diluted 1:10 and amplified with sequencing library adaper specific primer for 15 cycles inorder to obtain enough sequencing template. After purification enriched libraries were subjected to quality and quantity check with Agilent DNA High sensitivity BioAnalyzer kit (Agilent technologies, USA). The qualified libraries were used for template preparation using Ion PGM™ template OT2 200 kit in Ion one touch2 system. The templates were then enriched using Ion one touch ES. The enriched libraries were sequenced as single read sequencing with Ion PGM

sequencer using Ion PGMTM sequencing 200 kit v2 and 318 chip (Life technologies, USA) by following the manufacturer's instructions. 3) The sequenced reads (composed of A, C, T, or G was then processed to obtain a valid constant region and unique random region) were retained and split into separate files through unique 10-nt ion xpress-barcode using the Ion torrent suit 3.4.2 as mentioned before. To count the amount of PIP enriched unique DNA sequences, a sliding window of length k (=6) in MERMADE, a new pipeline for Bind-n-Seq analysis (http://korflab.ucdavis.edu/Data_sets/BindNSeq.27) were used. Highly enriched motifs were confirmed with DREME primary motif analysis.

SPR analysis

SPR analyses were performed as described in previous studies [13] using BIACORE X instrument.In brief, we purchased biotinylated hairpin DNAs with match and mismatch PIP binding sites from JBioS (Tokyo, Japan) (**7** and **9** match / **8** and **10** mismatch: Sequence in the promoter region of the gene encoding POU homeodomain [8] -5'-Biotin- GCG CCT TCC TTC CCC TTT TGG GGA AGG AAG GCG C-3'and **7** and **9** mismatch / **8** and **10** match: Sequence in the promoter region of the gene encoding PIWIL2[10] -5'-Biotin- CGT CCT TTC CAG CAG TTTTCT GCT GGA AAG GAC G-3'). The purchased DNAs were diluted to 100nM. Then immobilization of hairpin biotinylated DNAs was performed on a streptavidin-coated sensor chip SA to obtain the desired immobilization level (approximately 1100-1200 RU rise). HBS-EP buffer (10mMHEPES, pH 7.4, 150 mM NaCl, 3 mM EDTA, and 0.005% surfactant P20) with 0.1% DMSO at room temperature was used to carry out SPR assays. We prepared an order of **7-10** (without biotin) solutions with different concentrations in HBS-EP buffer with 0.1% DMSO and at the flow rate of 20 mL/min, the PIPs were passed on the immobilized oligonucleotide chips. The data processing was performed using BIAevaluation 4.1 program to measure the rates of association (k_a) and dissociation (k_d) and dissociation constant (K_D), with an appropriate fitting model.

Experimental procedures for synthesis and purification of polyamides and are given in supplementary information.

Received: ((will be filled in by the editorial staff))
Published online on ((will be filled in by the editorial staff))

Keywords: DNA recognition · High throughput screening · Next generation sequencing · synthetic biology

[1] M. Berdasco, M. Esteller, *Dev. cell* **2010**, *19*, 698-711.
[2] W. S. Wade, M. Mrksich, P. B. Dervan, *J. Am. Chem. Soc.* **1992**, *114*, 8783-8794.
[3] a) D. E.Wemmer, P. B. Dervan, *Curr. Opin. Struct. Biol.* **1997**, *7*, 355 – 361; b) P. B. Dervan, B. S. Edelson, *Curr. Opin. Struct. Biol.***2003**, *13*, 284 – 299.
[4] J. G. Pelton, D. E. Wemmer, *Proc. Natl. Acad. Sci. U.S.A.* **1989**, *86*, 5723−5727.
[5] T. Kouzarides, *Cell* **2007**, *128*, 693 – 705.
[6] A. Ohtsuki, M. T. Kimura, M. Minoshima, T. Suzuki, M. Ikeda, T. Bando, H. Nagase, K. ichi Shinohara, H. Sugiyama, *Tetrahedron Letters* **2009**, *50*, 7288–7292.
[7] a) G. N. Pandian, K. Shinohara, A. Ohtsuki, Y. Nakano, M. Masafumi, T. Bando, H. Nagase, Y. Yamada, A. Watanabe, N. Terada, S. Sato, H. Morinaga, H. Sugiyama, *ChemBioChem* **2011**, *12*, 2822 – 2828; b) G. N. Pandian, A. Ohtsuki, T. Bando, S. Sato, K. Hashiya, H. Sugiyama, *Bioorg. Med. Chem.* **2012**, *20*, 2656 – 2660; c) G. N. Pandian, Y. Nakano, S. Sato, H. Morinaga, T. Bando, H.Nagase, H. Sugiyama, *Sci. Rep.* **2012**, *2*, 544.
[8] G. N. Pandian, J. Taniguchi, S. Junetha, S. Sato, L. Han, A. Saha, C. AnandhaKumar, T. Bando, H. Nagase, T. Vaijayanthi, R. D. Taylor, H. Sugiyama, *Sci. Rep.* **2014**, *4*, 3843.
[9] a) Meier, J. L.; Yu, A. S.; Korf, I.; Segal, D. J.; Dervan, P. B. *J. Am. Chem. Soc.* **2012**, *134*, 17814-17822; b) J. S. Kang, J. L. Meier, P. B. Dervan, *J. Am. Chem. Soc.* **2014**, *136*, 3687-3694
[10] L. Han, G. N. Pandian, S. Junetha, S. Sato, C. Anandhakumar, J. Taniguchi, A. Saha, T. Bando, H. Nagase, H. Sugiyama, *Angew. Chem. Int. Ed.* **2013**, 13410-13413.
[11] A. Zykovich, I. Korf, D. J. Segal, *Nucleic acids research* **2009**, *37*, e151.
[12] a) T. L. Bailey, *Bioinformatics* **2011**, *27*, 1653–1659; b) C. T. Workman, Y. Yin, D. L. Corcoran, T. Ideker, G. D. Stormo, P. V. Benos, *Nucleic Acids Res.* **2005**, *33*, W389-392.
[13] H. Morinaga,T. Bando, T. Takagaki, M. Yamamoto, K. Hashiya, H. Sugiyama, *J. Am. Chem. Soc.* **2011**, *133*, 18924-18930.
[14] M. Minoshima, T. Bando, S. Sasaki, J. Fujimoto, H. Sugiyama, *Nucleic acids research* **2008**, *36*, 2889-2894.

*C. Anandhakumar, Y. Li, S. Kizaki, G. N. Pandian, K. Hashiya, T. Bando, H. Sugiyama** _____ **Page – Page**

Next-Generation Sequencing Studies Guide the Design of Pyrrole-Imidazole Polyamides with Improved Binding Specificity by the Addition of β-alanine

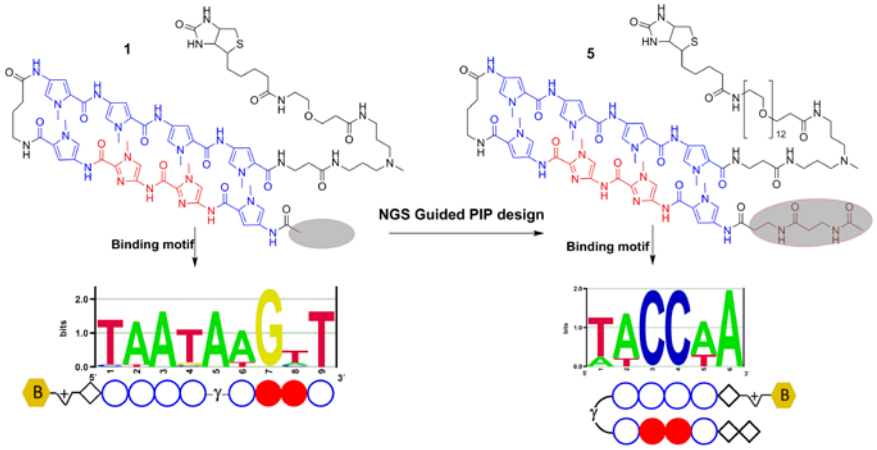

Small molecule design and screening guided by next-generation sequencing. The application of small molecules that bind to DNA in various systems depends highly on the binding affinity toward genome-scale sequence. DNA minor groove binders such as SAHA-PIPs have shown strong biological effects, but it was not clear whether the effects were due to their binding specificity. We therefore used a cost-effective method based on affinity purification and massively parallel sequencing to address this question. Binding-motif identification guided the redesign of polyamide derivatives and revealed the importance of ββ-moieties for enhanced binding of PIPs.

Supporting information

Table of contents

Synthesis of biotin-conjugated polyamides and polyamides used in SPR analysis

General scheme for Synthesis of biotin-conjugated

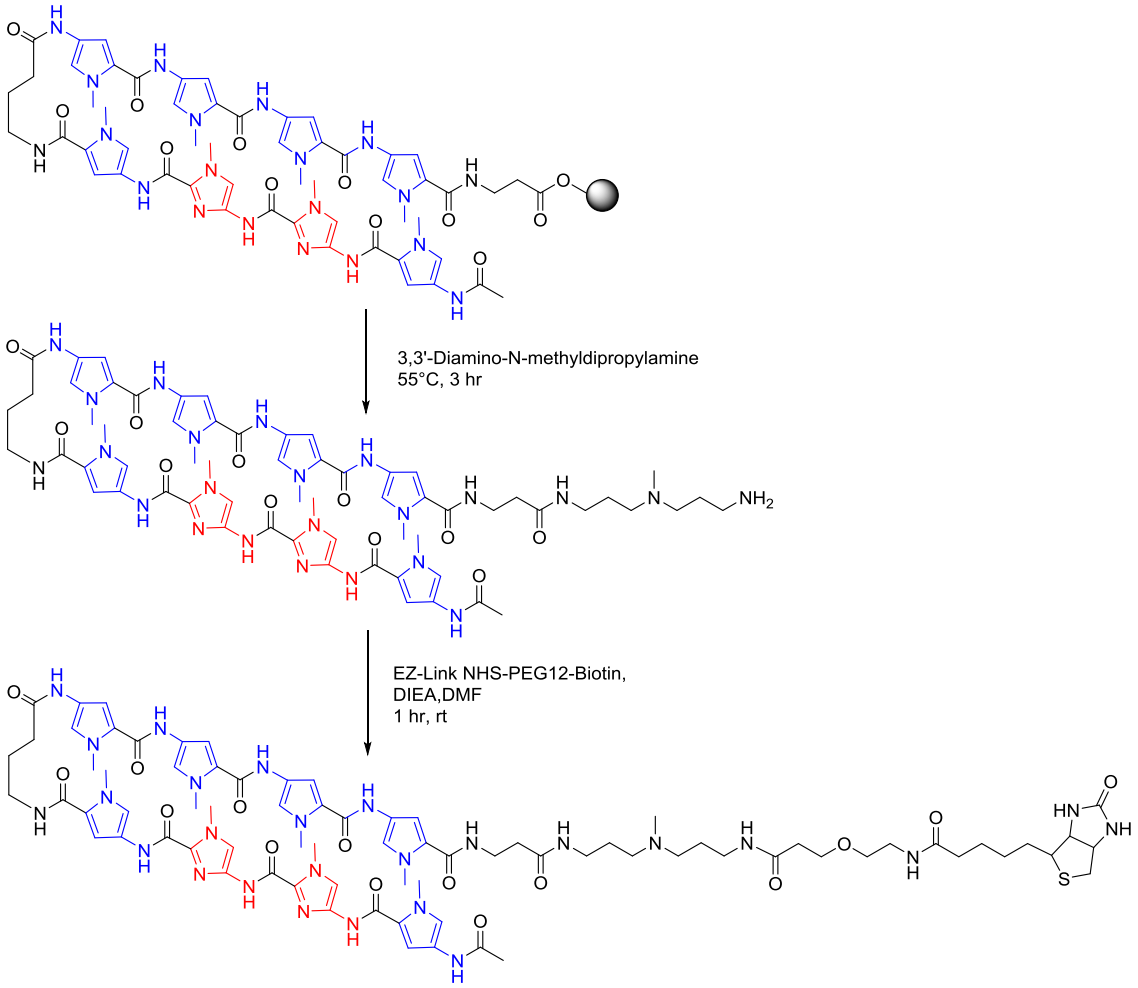

General

Reagents and solvents were purchased from standard suppliers and used without further purification. The EZ-Link NHS-PEG_{12}-Biotin was purchased from Thermo Scientific (number 21312).The analytical HPLC was performed with a COSMOSIL 5C18-MS-II reversed phase column (4.6×150 mm, Nacalai) in 0.1% TFA in water with CH_3CN as eluent at a flow rate of 1.0 mL/min, and a linear gradient elution of 0−100% CH_3CN over 20 min or 40 min with detection at 254 nm. The HPLC purification was performed with a COSMOSIL 5C18-MS-II reversed phase column (10 ×150 mm, Nacalai) in 0.1% TFA in water with CH_3CN as eluent. The final products were analyzed by ESI-TOF-MS (Bruker).

Ac-Py-Im-Im-Py-γ-Py-Py-Py-Py-β-(+)-PEG$_{12}$-Biotin (1)

Py-Im polyamide supported by oxime resin was prepared in a stepwise reaction by a reported Fmoc solid-phase procedure. The product with oxime resin was cleaved with 3,3'-Diamino-*N*-methyldipropylamine (500μL) at 55℃ for 3 hours. After filtration and evaporation, the resulted oil was quenched by Et_2O. The obtained precipitation was washed with Et_2O for three times and dried in vacuo. The product was used for the next coupling steps without further purification.

A solution of polyamide (1.32 mg, 1μmol), EZ-Link NHS-PEG$_{12}$-Biotin (1mg, 1.2 μmol) and DIEA (2 μL, 10 μmol) in DMF (100 μL) was stirred at room temperature for 1 hour. After consumption of starting material was confirmed by HPLC, Et_2O was added to the mixture and the resultant was collected by centrifugation, and washed by Et_2O and CH_2Cl_2. The crude product was purified by reverse-phase HPLC. After lyophilization **1** was obtained (0.9 mg, yield 42%). Analytical HPLC: t_R= 15.5 min (0.1% TFA-CH_3CN, 0−100%, 40min). ESI-TOF-MS m/z: calcd for $C_{99}H_{146}N_{26}O_{26}S$ $[M+2H]^{2+}$ 2149.0622, found 2149.0460.

Ac-Im-Im-Py-Py-γ-Py-Py-Py-Py-β-(+)-PEG$_{12}$-Biotin (2)

A similar synthetic procedure of **1** was used for the preparation of **2**. Analytical HPLC: t_R= 15.7 min (0.1% TFA-CH_3CN, 0−100%, 40min). ESI-TOF-MS m/z: calcd for $C_{99}H_{146}N_{26}O_{26}S$ $[M+2H]^{2+}$ 2149.0622, found 2149.1082.

SAHA-β-β-Py-Im-Im-Py-γ-Py-Py-Py-Py-β-(+)-PEG$_{12}$-Biotin (3)

A similar synthetic procedure of **1** was used for the preparation of **3**. Analytical HPLC: t_R= 17.2 min (0.1% TFA-CH_3CN, 0−100%, 40min). ESI-TOF-MS m/z: calcd for $C_{119}H_{173}N_{29}O_{31}S$ $[M+2H]^{2+}$ 2538.2573, found 2538.0851.

SAHA-β-β-Im-Im-Py-Py-γ-Py-Py-Py-Py-β-(+)-PEG$_{12}$-Biotin (4)

A similar synthetic procedure of **1** was used for the preparation of **4**. Analytical HPLC: t_R= 17.3 min (0.1% TFA-CH_3CN, 0−100%, 40min). ESI-TOF-MS m/z: calcd for $C_{119}H_{173}N_{29}O_{31}S$ $[M+2H]^{2+}$ 2538.2573, found 2538.2536.

Ac-β-β-Py-Im-Im-Py-γ-Py-Py-Py-Py-β-(+)-PEG$_{12}$-Biotin (5)

A similar synthetic procedure of **1** was used for the preparation of **5**. Analytical HPLC: t_R= 9.1 min (0.1% TFA-CH_3CN, 0−100%, 20min). ESI-TOF-MS m/z: calcd for $C_{105}H_{156}N_{28}O_{28}S$ $[M+2H]^{2+}$ 2291.1365, found 2290.8420.

Ac-β-β-Im-Im-Py-Py-γ-Py-Py-Py-Py-β-(+)-PEG$_{12}$-Biotin (6)

A similar synthetic procedure of **1** was used for the preparation of **6**. Analytical HPLC: t_R= 9.1 min (0.1% TFA-CH_3CN, 0−100%, 20min). ESI-TOF-MS m/z: calcd for $C_{105}H_{156}N_{28}O_{28}S$ $[M+2H]^{2+}$ 2291.1365, found 2290.8356.

Oligomer sequences used in Bind-n-Seq method (referenced in experimental section in main text)

Bind-n-Seq 92mer:

5'CCATCTCATCCCTGCGTGTCTCCGACTCAGXXXXXXXXXXNNNNNNNNNNAATCACCGACTGCCCATA

GAGAGGAAAGCGGAGGCGTAGTGG 3`

• All barcoded Bind-n-Seq 92 mers were synthesized by Sigma Aldrich machine mixing, standard desalting purification.

• Barcode in yellow shadow (XXXXXXXXXX), 10-letter barcodes used as per Ion torrent sequencing technologies.

Primer 1:

5`-CCA CTA CGC CTC CGC TTT CCT CTC TA-3`

• Used in initial primer extension reaction.

• Synthesized by Sigma Aldrich, purification by standard desalting.

General scheme for synthesis of polyamides used for SPR analysis

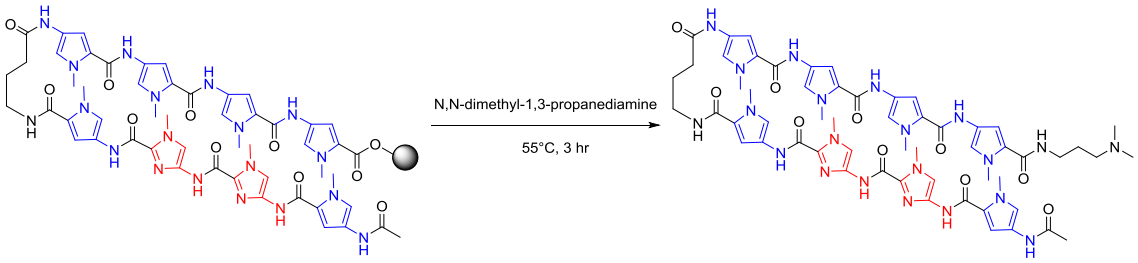

Ac-Py-Im-Im-Py-γ-Py-Py-Py-Py-Dp (7)

Py-Im polyamide supported by oxime resin was prepared in a stepwise reaction by a reported Fmoc solid-phase procedure. The product with oxime resin was cleaved with *N*,*N*-dimethyl-1,3-propanediamine (500μL) at 55℃ for 3 hours. After filtration and evaporation, the resulted oil was quenched by Et_2O. The obtained precipitation was washed with Et_2O for three times and dried in vacuo. The crude product was purified by reverse-phase HPLC. Analytical HPLC: t_R= 9.0 min (0.1% TFA-CH_3CN, 0−100%, 20min). ESI-TOF-MS m/z: calcd for $C_{57}H_{69}N_{21}O_{10}$ $[M+2H]^{2+}$ 1209.5536, found 1209.3718.

Ac-Im-Im-Py-Py-γ-Py-Py-Py-Py-Dp (8)

A similar synthetic procedure of **7** was used for the preparation of **8**. Analytical HPLC: t_R= 9.4 min (0.1% TFA-CH_3CN, 0−100%, 20min). ESI-TOF-MS m/z: calcd for $C_{57}H_{69}N_{21}O_{10}$ $[M+2H]^{2+}$ 1209.5536, found 1209.4150.

Ac-β-β-Py-Im-Im-Py-γ-Py-Py-Py-Py-Dp (9)

A similar synthetic procedure of **7** was used for the preparation of **9**. Analytical HPLC: t_R= 9.2 min (0.1% TFA-CH_3CN, 0−100%, 20min). ESI-TOF-MS m/z: calcd for $C_{63}H_{79}N_{23}O_{12}$ $[M+2H]^{2+}$ 1351.6279, found 1351.5146.

Ac-β-β-Im-Im-Py-Py-γ-Py-Py-Py-Py-Dp (10)

A similar synthetic procedure of **7** was used for the preparation of **10**. Analytical HPLC: t_R= 9.2 min (0.1% TFA-CH_3CN, 0−100%, 20min). ESI-TOF-MS m/z: calcd for $C_{63}H_{79}N_{23}O_{12}$ $[M+2H]^{2+}$ 1351.6279, found 1351.5112.

SUPPLEMENTARY FIGURES

Figure S1.

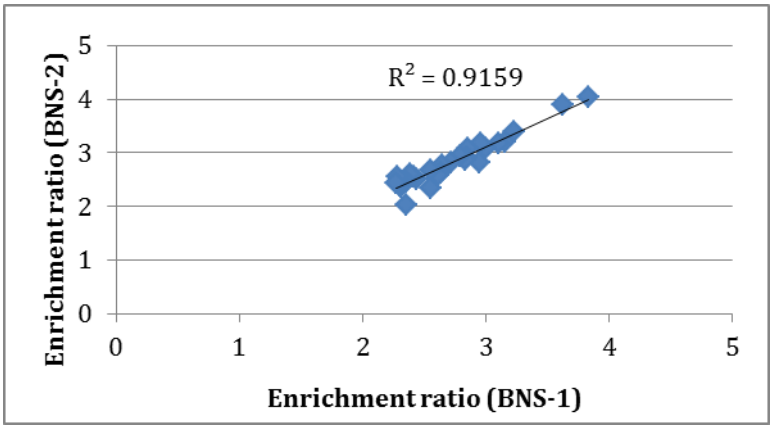

Figure S1, Graphical representation of relative enrichment of two separate binding and enrichment reactions of **3** (sequence details are provided in S.Table 1)

Figure S2

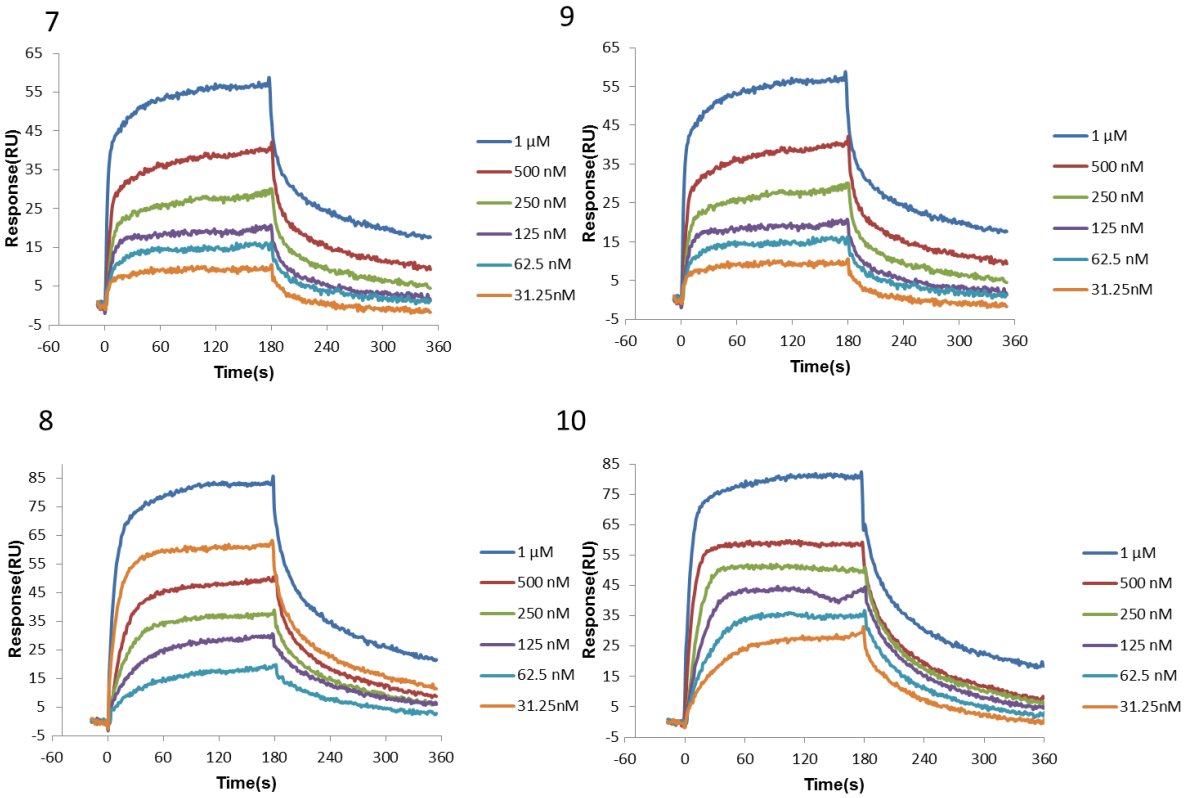

Figure S2, SPR sensorgrams for the interactions of **7** and **9** with its match and **8** and **10** with its mismatch binding sequences in the promoter region of the gene encoding POU homeodomain (Binding specificities were provided in main text table.1) are shown.

Figure. S3

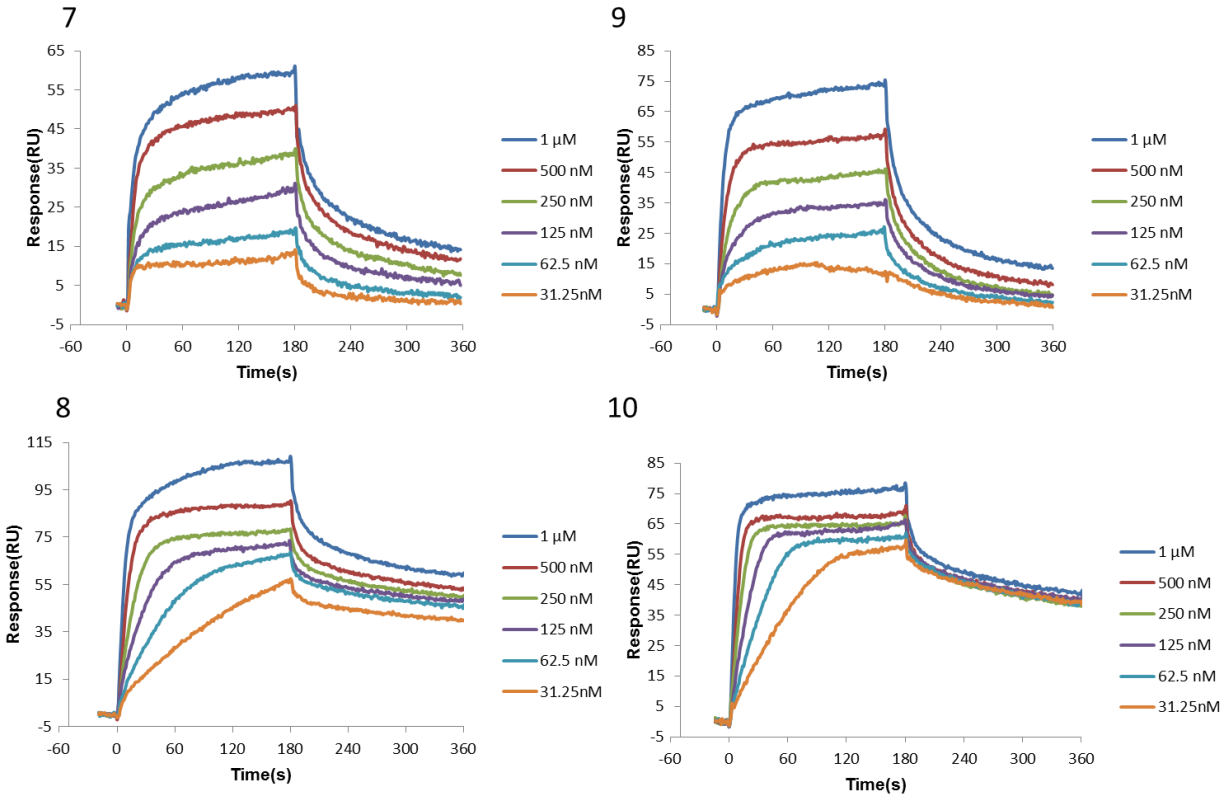

Figure S3, SPR sensorgrams for the interactions of compounds **7** and **9** with its mismatch and **8** and **10** with its match binding sequences in the promoter region of the gene encoding PIWIL2 (Binding specificities were provided in main text table.1) are shown.

SUPPLEMENTARY TABLES

Table S1: Relative enrichment of 6-base pair "k"mers enriched by **3** in two separate binding and enrichment reactions (only top 30 sequences were shown). Its corresponding graph were shown in Figure S1.

Rank	Sequences	Enrichment ratio (BNS-1)	Enrichment ratio (BNS-1)
1	TACCAA	3.83	4.047
2	ATTACC	3.63	3.89
3	GGTACC	3.231	3.393
4	CTACCA	3.155	3.2
5	GTACCA	3.109	3.166
6	TGGTAA	3.006	3.085
7	AACCAA	2.959	3.169
8	ATGGTA	2.945	2.812
9	AATACC	2.853	3.083
10	ATACCA	2.846	2.918
11	GGTAGA	2.831	2.863
12	TTCCAA	2.795	2.931
13	CTTCCA	2.721	2.827
14	ACCAAT	2.651	2.779
15	GTTCCA	2.634	2.616
16	GGTACA	2.617	2.574
17	AGGTAG	2.559	2.675
18	ACCATC	2.55	2.331
19	CCAACC	2.439	2.503
20	GGAAGA	2.416	2.561
21	ATAACC	2.383	2.59
22	GGAACC	2.359	2.468
23	CCATCC	2.352	2.024
24	AACCAT	2.316	2.369
25	ACCAAG	2.313	2.46
26	GAACCA	2.308	2.38
27	ACTTCC	2.303	2.456
28	ACTACC	2.285	2.442
29	ACCAAC	2.279	2.547
30	AGGTAC	2.276	2.426

Table S2: Relative enrichment of 6-base pair “k”mers enriched by **4** binding and enrichment reactions.

Rank	Sequence	Enrichment
1	TTACCA	4.26
2	ATTACC	3.822
3	AATGGT	3.454
4	ATAACC	3.37
5	ATGGTA	3.205
6	ATTGGT	2.916
7	TAACCA	2.783
8	TTGGTA	2.631
9	TATGGT	2.568
10	CTTACC	2.352
11	ATACCA	2.286
12	ATATGG	2.267
13	GTTACC	2.246
14	TATTGG	2.231
15	TAATGG	2.185
16	AATTGG	2.105
17	TATACC	2.086

Table S3: Relative enrichment of 6-base pair "k"mers enriched by **5** binding and enrichment reactions. (only top 30 sequences were shown).

Rank	Sequence	Enrichment
1	TACCAA	3.635
2	ATTACC	3.585
3	CTACCA	2.993
4	TGGTAA	2.785
5	GTACCA	2.982
6	AACCAA	2.745
7	ATGGTA	2.754
8	TACCTA	2.325
9	ACTACC	2.541
10	GGTAGA	2.641
11	ATACCA	2.693
12	ACCAAT	2.539
13	CTTCCA	2.531
14	ACCAAC	2.197
15	GGTACA	2.393
16	TTCCAA	2.513
17	AGGTAG	2.568
18	GTTCCA	2.363
19	AATACC	2.722
20	CAACCA	2.085
21	GGAAGA	2.335
22	ACCAAG	2.215
23	AAGGTA	2.208
24	AGTACC	2.256
25	ATAACC	2.224
26	GAACCA	2.089
27	ACTTCC	2.232
28	ACCTAC	2.034
29	AGGTAC	2.234
30	ACCATC	2.445

Table S4: Relative enrichment of 6-base pair “k”mers enriched by **6** binding and enrichment reactions.

Rank	Sequence	Enrichment
1	AATGGT	3.147
2	TTACCA	3.142
3	ATGGTA	2.851
4	ATTACC	2.835
5	ATAACC	2.476
6	ATTGGT	2.395
7	TTGGTA	2.338
8	TAATGG	2.148
9	TATGGT	2.126
10	TAACCA	2.101